Özdenkçi, Karhan; De Blasio, Cataldo; Sarwar, Golam; Melin, Kristian; Koskinen, Jukka; Alopaeus, Ville

Techno-economic feasibility of supercritical water gasification of black liquor

Published in:
Energy

DOI:
10.1016/j.energy.2019.116284

Published: 15/12/2019

Document Version
Peer-reviewed accepted author manuscript, also known as Final accepted manuscript or Post-print

Techno-Economic Feasibility of Supercritical Water Gasification of Black Liquor

Karhan Özdenkçi[1,*], Cataldo De Blasio[2], Golam Sarwar[1], Kristian Melin[3], Jukka Koskinen[1], Ville Alopaeus[1]

1. Department of Chemical and Metallurgical Engineering, Aalto University, Espoo, Finland
2. Faculty of Science and Engineering, Energy Technology, Åbo Akademi University, Vaasa, Finland
3. VTT, Technical Research Center of Finland, Espoo, Finland
* Corresponding author: karhan.ozdenkci@aalto.fi

Abstract: The objective of this study is to investigate the techno-economic feasibility of supercritical water gasification (SCWG) of black liquor integrated to a Kraft pulp mill. The process simulations have been performed through Aspen Plus software. The assessment includes five integration scenarios: stainless steel 316 or Inconel 625 as the reactor materials and hydrogen or combined heat and power (CHP) as the target products. The results illustrates that Inconel reactor is more profitable for CHP production than stainless steel as well as providing lower production cost of hydrogen. Inconel is also more robust against loss of pulping chemicals and changes in the energy price. However, the assessment uses the experimental yields even though surface-to-volume ratio of the reactor will reduce in the industrial scale. Therefore, the results should be validated in pilot scale as well before implementation. Nevertheless, a special reactor configuration can increase surface area. The techno-economic results can be improved by comprehensive investigations of process conditions including also residence time, the concentration of reactor inlet and heterogeneous catalyst. In addition, the SCWG process integrated to a pulp mill can also receive feedstocks from other biomass sectors. This would improve the economic and environmental performances of those sectors as well.

Keywords: supercritical water gasification, black liquor, integrated biorefinery, feasibility, hydrogen production, process simulation, techno-economic assessment

1. Introduction

The importance of biomass has increased due to the environmental issues and fossil fuel depletion. Rather than 1st generation biorefinery, the sustainable industry could include integrated processes utilizing non-edible crops or waste and by-product streams. However, this requires advanced technologies currently in need of further investigations and techno-economical improvements. The main conversion routes include pyrolysis and gasification processes followed by the production of various fuels and chemicals [1,2]. In addition, electrochemical conversion is another method to produce platform chemicals [3–5].

As a major biomass sector, pulp and paper industry provides green energy and a potential for multi-product biorefinery. For instance, black liquor combustion consists of 12 % of the whole combined heat and power (CHP) generation in Finland in 2014 [6]. The commercial treatment includes evaporation followed by recovery boiler. However, this treatment has operational issues despite being feasible for wood mills. The energy-demanding evaporation step is the main issue the commercial treatment. Furthermore, this treatment is unsuitable for non-wood mills. Silica content of non-wood black liquor causes too high viscosity to transfer when concentrating to sufficient concentration for the recovery boiler. The maximum limit for proper flowability is around 50 % solid content; however, the recovery boiler then becomes inefficient. In addition, there are also market issues driving pulp mills to be evolved into multi-product plants: decreasing demand for printing paper and the "green" production becoming more important. An industrial implementation involves the lignin recovery through acidification of black liquor [7]. In addition, prior partial wet oxidation (PWO) reduces the filtration resistance without altering the material quality, known as LignoForce process [8]. The most investigated alternative include black liquor gasification [9]. Then, the syngas can be processed to produce electricity, motor fuels or dimethyl ether [10]. However, despite slight increase in power efficiency compared to the recovery boiler treatment, gasification also requires evaporation as a prior step. The efficiency of a gasifier increases with decreasing moisture content of inlet stream, thus requiring an intensive feed stream drying [11]. From the economic viewpoint, moisture content of biomass feedstock increases the production cost of electricity via drying followed by gasification [11]. Similarly, an exergy analysis pinpointed the evaporation step as the main source of exergy loss for thermal processes and reported higher exergy efficiencies for hydrothermal processes [12]. For instance, supercritical water gasification (SCWG) becomes more efficient than gasification process when the feedstock moisture is more than 30 % [13]. Therefore, hydrothermal processes are more effective for wet biomass. Similarly, hydrothermal liquefaction (HTL) produces bio-oil with less oxygen content compared to pyrolysis, thus requiring less hydrogen for upgrading [14]. As another alternative, PWO of black liquor can produce carboxylic acids or salts of these acids [15]. However, separation of each acid or salt becomes challenging due to dilute streams [16].

SCWG is a potentially suitable process for by-products of a pulp mill, e.g. black liquor [17–19], black liquor mixed with wheat straw [20] and paper sludge [21]. Supercritical water becomes an effective solvent for organics and gases [22]. The reaction rates become faster as well with the dominance of radical mechanism at high temperature; for instance, depolymerization reactions occur instantly [23,24]. However, SCWG has plugging issue due to the negligible solubility of inorganic salts. Nevertheless, a suitable reactor configuration can provide an opportunity for the recovery of pulping chemicals in the solid residue. Regarding the technology readiness level, SCWG has reached to the pilot scale for other types of biomass than black liquor: VERENA pilot plant, a pilot plant in Hiroshima and another plant in Pacific Northwest Laboratory with the capacities of 2.4, 1 and 0.6 ton of wet biomass per day, respectively [25,26]. In addition, there is also PSI (Paul Scherrer Institute) process with the

capacity of 24 kg per day, recently being upscaled 1.2 tons per day [27]. This process involves a salt separator followed by a reactor with fixed bed Ru/C catalyst. However, reaching commercialization requires further improvements to reduce production costs and techno-economic assessments for various biomass feedstocks.

Integrating SCWG of black liquor can improve the profitability of a pulp mill. The recent studies reported promising yields of syngas [17,19]. The impact analysis of conditions pinpointed temperature as the most influential parameter followed by residence time and feed concentration [17]. Even though residence time is expected to improve the yields [19], long residence time at high temperature can cause repolymerization, thus increasing char formation, as well as increasing the reactor cost [28]. From the techno-economic assessment viewpoint, moderate level of residence time is at the interest to design a feasible process in terms of reactor costs and promising gas yields.

The purpose of this study is to determine the feasibility of SCWG of black liquor integrated with a pulp mill. The SCWG process is designed by using the experimental data presented in a previous study [17]. Five different scenarios are investigated based on two reactor materials and syngas target products: combined heat and power (CHP) production or H_2 production in an Inconel 625 or a stainless steel 316 reactor.

2. Process Description and Simulation of the Scenarios

This study investigates the integration of SCWG to a Kraft mill with the capacity of 400 000 air-dried tons of (ADt) pulp per year. The mill is assumed to produce 10 tons of weak Kraft black liquor (KBL) per ADt pulp. Transferring 20 % of weak KBL results in the SCWG plant capacity of 100 t/h weak black liquor inlet. Table 1 summarizes the integration case. Table 2 presents the main properties of weak KBL.

Table 1. The pulp mill and the integration case

The pulp mill capacity	400 000 ADt / year
The weak black liquor amount	4 Mton / year
The fraction of KBL to SCWG plant	20 %
Annual operation duration	8000 h / year
The SCWG plant capacity	800 ktons weak BL inlet / year 100 t weak BL inlet / h 22.8 t dry solid intet / h

Table 2. Properties of weak KBL

Organic content	14.7 wt-%
Ash Content	8.1 wt-%
Sodium	18.36 g/kg KBL
Sulphur	8.26 g/kg KBL
LHV	14.4 MJ/kg dry basis
Moisture content	77.2 wt-%

2.1. Integration Scenarios

The basis for the process design include experimental data at temperature range of 500-700 °C and 25 MPa, with residence time of 1.3-1.9 minutes (constant inlet volumetric flow rate, residence time varying slightly with temperature) and in Inconel 625 and stainless steel 316 reactors [17]. SCWG process can be integrated with the target product of CHP or hydrogen. The reaction temperature is selected to maximize hot gas efficiency for CHP production and to maximize hydrogen yield for hydrogen production. In addition, a scenario of Inconel reactor is added at 700 °C as a hydrogen production scenario because of higher thermal efficiency resulting in higher revenue through off-gas, despite lower hydrogen yield than the scenario of Inconel reactor at 600 °C. Furthermore, although Inconel gives higher yields, stainless steel is a cheaper material. Therefore, it is worth to investigate both reactor materials from the economic viewpoint. Table 3 presents the scenarios.

Table 3. The scenarios of SCWG plant integration

Scenarios	**Target product**	**Reactor material**	**Reactor temperature**
CHP-Inc-700	CHP	Inconel 625	700 °C
CHP-SS-700	CHP	Stainless steel 316	700 °C
H2-Inc-600	Hydrogen	Inconel 625	600 °C
H2-Inc-700	Hydrogen	Inconel 625	700 °C
H2-SS-700	Hydrogen	Stainless steel 316	700 °C

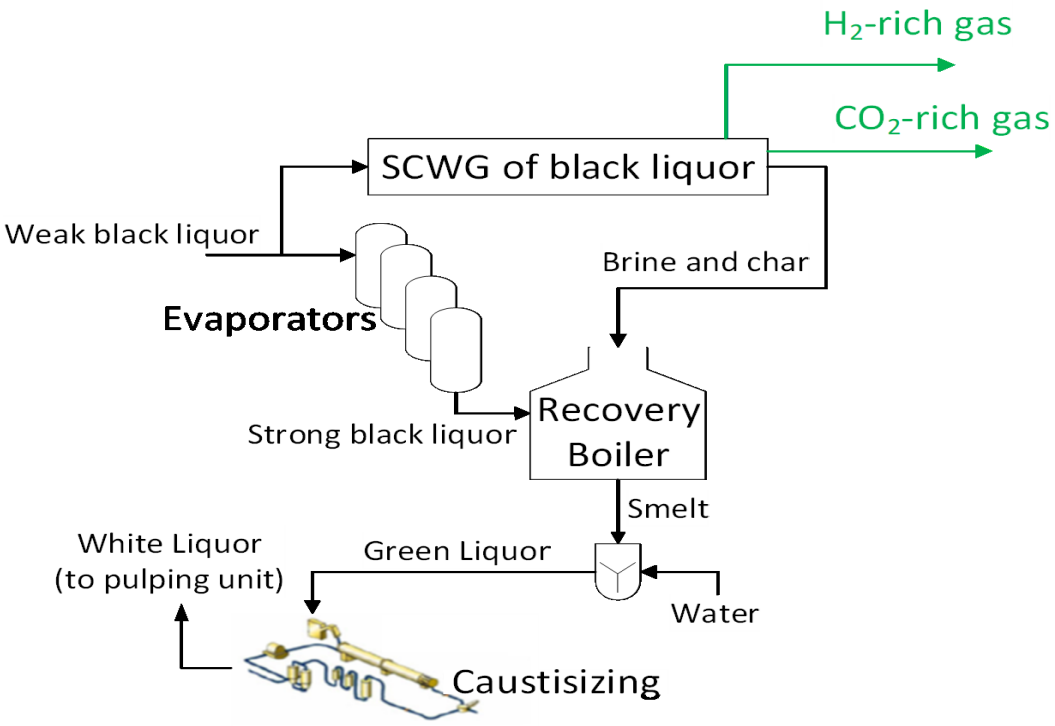

Figure 1. The integration of SCWG to a pulp mill

SCWG process can convert part of the weak black liquor into syngas, defined as 20 % in this study. The brine and char residue can be recycled to the recovery boiler to enable the recovery of pulping chemicals and to recover the energy stored in char. Figure 1 shows the integration of SCWG to a pulp mill. The integration to a pulp mill leads to certain advantages regarding infrastructure:

- the gas engines and turbines of the mill utilized for CHP production
- flue gas from the recovery boiler utilized for heating to high temperature
- the excess heat to be utilized or sold

2.2. Process Simulation in Aspen Plus

Aspen Plus simulation requires feedstock definition, yields and thermodynamic methods. The stream class is defined as “MIXNC”. The non-conventional solid (NC Solid) components include lignin, ash and char. The enthalpy and density methods are defined as “HCOALGEN” (with all optional codes of 1) and “DCOALIGT”, respectively. These methods being originally suggested for coal would not cause significant errors since the organic part is mostly lignin and streams are very dilute.

Table 4 gives the weak black liquor components and flow rates. Table 5 gives the analysis of non-conventional components. Temperature and pressure of the feed black liquor are defined as 175 °C and 11 bars. The thermodynamic method is defined as “SRK” equation of state and “STEAMNBS” for water properties. SRK is suitable for high-pressure systems with lean liquid streams, as listed also one of the suitable options in the selection guide of Aspen Plus. Then, it

is recommended to use NBS tables for water properties when using SRK equation of state. The "RYIELD" type of reactor is used in the simulation. Table 6 gives yields in the reactor per non-inert inlet, and ash is defined as the only inert.

Table 4. Feed stream components and flow rates

Mixed		**NC Solid**	
Component	**Flow rate (kg/h)**	**Component**	**Flow rate (kg/h)**
Glucose	48	Lignin	13664
Galactose	201	Char	1
Arabinose	165	Ash	8073
Xylose	414		
Mannose	187		
Water	77247		

Table 5. Analysis of non-conventional components

	Lignin	**Char**	**Ash**
Ultimate			
Carbon	48.5	60	0.04
Hydrogen	6.4	5	0
Oxygen	45.1	35	25
Sulphur	0	0	10
Ash	0	0	64.96
Sulphur			
Pyritic	0	0	5
Sulfate	0	0	5
Organic	0	0	0
Proximate			
Fixed carbon	48.6	65	0
Volatile matter	51.5	35	0
Ash	0	0	100

Table 6. The reactor yields as mass/mass non-inert

	CHP-Inc-700	**CHP-SS-700**	**H2-Inc-600**	**H2-Inc-700**	**H2-SS-700**
H_2	2.495×10^{-3}	2.483×10^{-3}	2.979×10^{-3}	2.495×10^{-3}	2.483×10^{-3}
CO_2	3.040×10^{-2}	3.437×10^{-2}	2.782×10^{-2}	3.040×10^{-2}	3.437×10^{-2}
CH_4	7.748×10^{-3}	6.205×10^{-3}	4.746×10^{-3}	7.748×10^{-3}	6.205×10^{-3}
CO	1.344×10^{-4}	1.048×10^{-4}	1.239×10^{-4}	1.344×10^{-4}	1.048×10^{-4}
C_2H_6	2.282×10^{-3}	1.705×10^{-3}	9.769×10^{-4}	2.282×10^{-3}	1.705×10^{-3}
C_2H_4	1.495×10^{-4}	1.242×10^{-4}	2.251×10^{-4}	1.495×10^{-4}	1.242×10^{-4}
H2O	9.010×10^{-1}	8.983×10^{-1}	9.011×10^{-1}	9.010×10^{-1}	8.983×10^{-1}
char	9.011×10^{-3}	9.835×10^{-3}	1.454×10^{-2}	9.011×10^{-3}	9.835×10^{-3}

3. Material and Energy Balances

The process concepts are similar for all the scenarios. The weak black liquor cannot be heated to supercritical temperature of water prior to the reactor due to the issue of inorganic salt deposition in pipelines. Therefore, the weak black liquor and the recycled liquid are fed separately to the reactor. The reactor operates adiabatically by adjusting temperature of recycled liquid so that the mixture of these two inlets result in temperature slightly above the reaction temperature to compensate the endothermic reaction enthalpies. Nevertheless, this temperature variation is only around 15 °C. The recycled liquid can be heated with flue gas, e.g. a pipeline into the recovery boiler then back to the reactor. The separation involves two steps: high-pressure separation to recover H_2-rich gas and low-pressure separation to recover CO_2-rich gas. Then, H_2-rich gas goes through pressure swing adsorption (PSA) for the hydrogen production scenarios.

3.1. CHP Production Scenarios

The CHP production scenarios aim at maximizing the heating value of H_2-rich gas outlet. The temperature of high-pressure phase separation plays a vital role in this aim and the overall heat integration of the process. High temperature causes lower mass fraction of combustibles in higher flow rate of H_2-rich gas due to increasing solubility of gases and vapor pressure with temperature. Therefore, low temperature of 45 °C is selected for high-pressure phase separation.

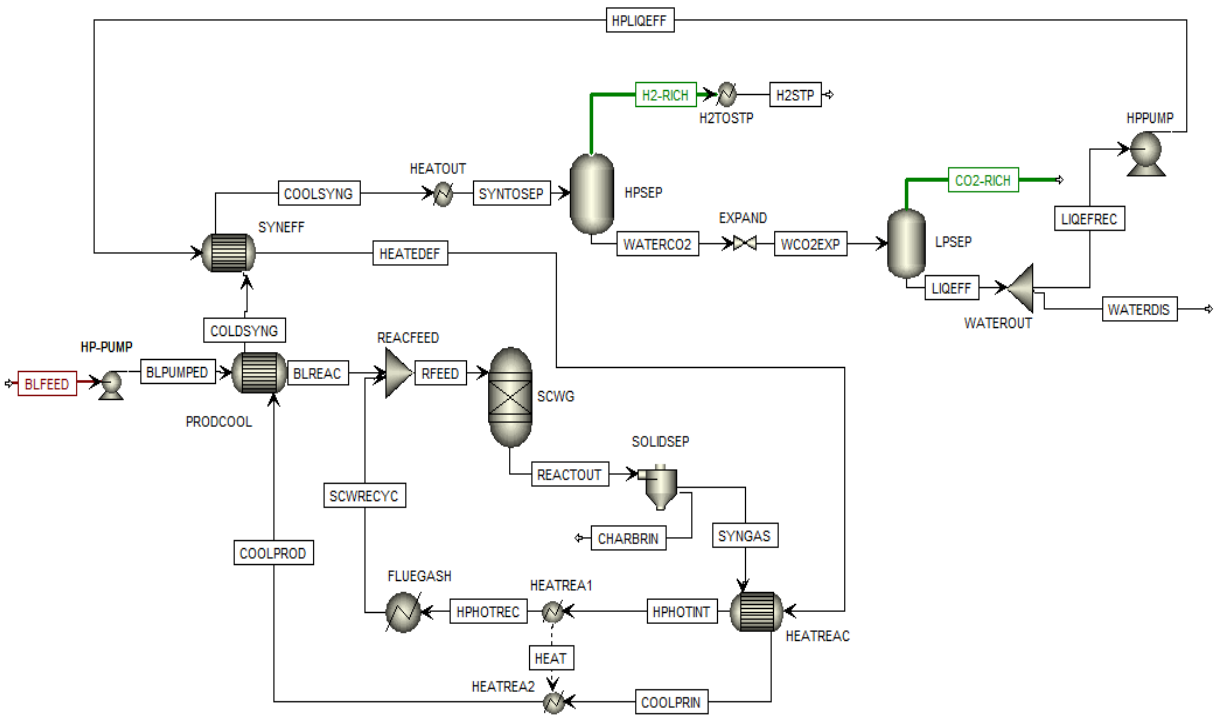

Figure 2. Process simulation of the CHP production scenarios

Figure 2 shows the process flow diagram of the energy production scenarios. The inlet "BLFEED" stream represents the weak black liquor received from the pulp mill. The outlet streams are "H2RICH" and "CO2RICH" gases and "CHARBRIN" solid as well as "WATERDIS" liquid. The stream of "H2STP" has an illustrative purpose to determine enthalpy difference between the outlet and the standard states. The energy inlet in the unit "FLUEGASH" heats the recycling liquid to 1000 °C by using flue gas. The temperature is selected to adjust heat duty of the reactor "SCWG" to zero. This energy inlet is assumed to have as CHP due to high temperature reached via flue gas. The stream "RFEED" has an illustrative purpose to observe the mixture temperature of black liquor and the recycling liquid. The energy outlet from the unit "HEATOUT" is district heat, cooling the high-pressure separation inlet. The pumps "HP-PUMP" and "HPPUMP" pressurize the black liquor feed and recycling liquid to 255 bars, respectively. The extra five bars is assumed for the pressure losses in the pipelines and the units. In the simulation, the reactor is represented with "RYIELD" reactor namely "SCWG" and solid removal with "SSPLIT" unit namely "SOLIDSEP".

The heat integration plays a critical role to reduce the external energy need. The "SYNGAS" stream heats the "HEATEDEF" stream. In Aspen, HeatX type of unit does not allow crossing over the critical temperature whereas Heater unit can simulate this cross over. Therefore, the heat exchange between "SYNGAS" and HEATEDEF" streams are simulated in two stages. First, "HPHOTINT" stream is set to 365 °C in the unit "HEATREAC". Then, "HPHOTREC" temperature is set to 680 °C in the unit "HEATREA1" and the heat of this unit is transferred to "HEATREA2" where the syngas is further cooled. The heat exchanger "PRODCOOL" heats the black liquor feed with "COOLPROD" stream. Similarly, the heat exchanger "SYNEFF" heat the recycling liquid. In these heat exchangers, the specification is defined as 20 °C temperature difference between hot inlet and cold outlet.

Figure 3 shows the input-output diagram for the energy production scenarios. The heating value of H2-rich gas is determined as the lower heating value (LHV) plus the enthalpy difference in the "H2TOSTP" unit. The energy output in "HEATOUT" units is assumed as district heat due to low temperature of the upstream. The heating value of H_2-rich gas is higher for the CHP-Inc-700 scenario because of higher gas yields.

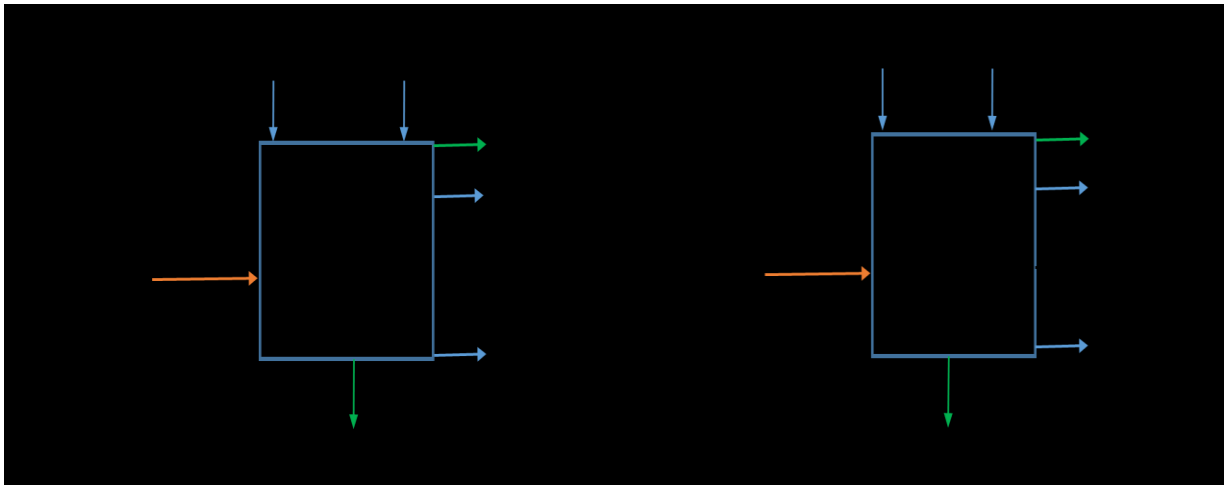

Figure 3. Input-output diagram for the energy production scenarios

3.2. Hydrogen Production Scenarios

Similar to energy production scenarios, low temperature favors the hydrogen amount in H_2-rich gas. Therefore, the lowest possible temperature is selected for the high-pressure phase separation, i.e. 45 °C.

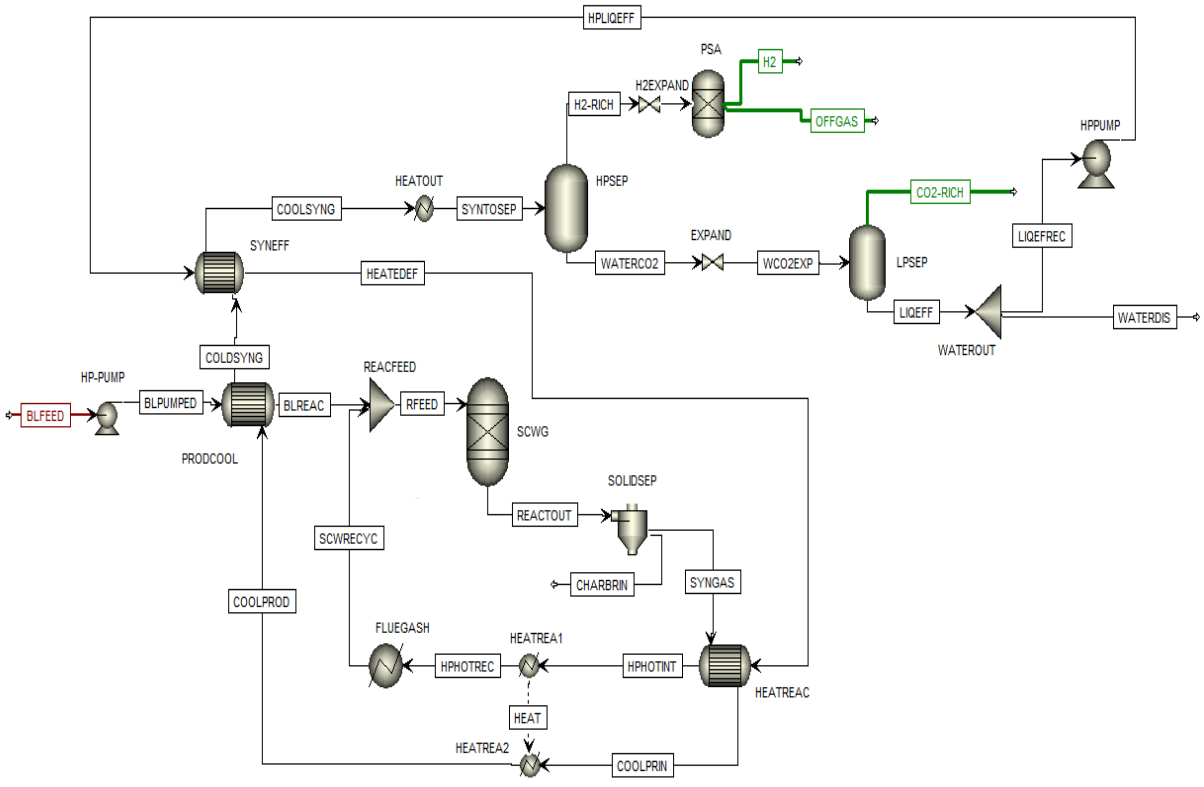

Figure 4. Process simulation of the hydrogen production scenarios

Figure 4 shows the process flow diagram of the hydrogen production scenarios. The process description is the same with the energy production scenarios, except H_2-rich gas going through PSA for hydrogen purification. The recycling liquid “SCWRECYC” is heated up to 1001 °C

for H2-SS-700 and H2-Inc-700 scenarios and to 866 ºC for H2-Inc-600 scenario to adjust heat duty in the reactor "SCWG" to zero. In addition, the same heat integration is applied for the hydrogen production scenarios as well. "HPHOTREC" temperature is set to 680 °C for the H2-SS-700 and H2-Inc-700 scenarios and to 580 ºC for the H2-Inc-600 scenario.

Figure 5 shows the input-output diagram for the hydrogen production scenarios. The energy input and outputs are the lowest for the H2-Inc-600 scenario due to lower temperature. Nevertheless, the hydrogen gas outlet is significantly higher in the H2-Inc-600 than the other two scenarios due to higher yields. The other two scenarios result in similar hydrogen yield whereas the H2-Inc-700 scenario provides the highest CHP production through off-gas.

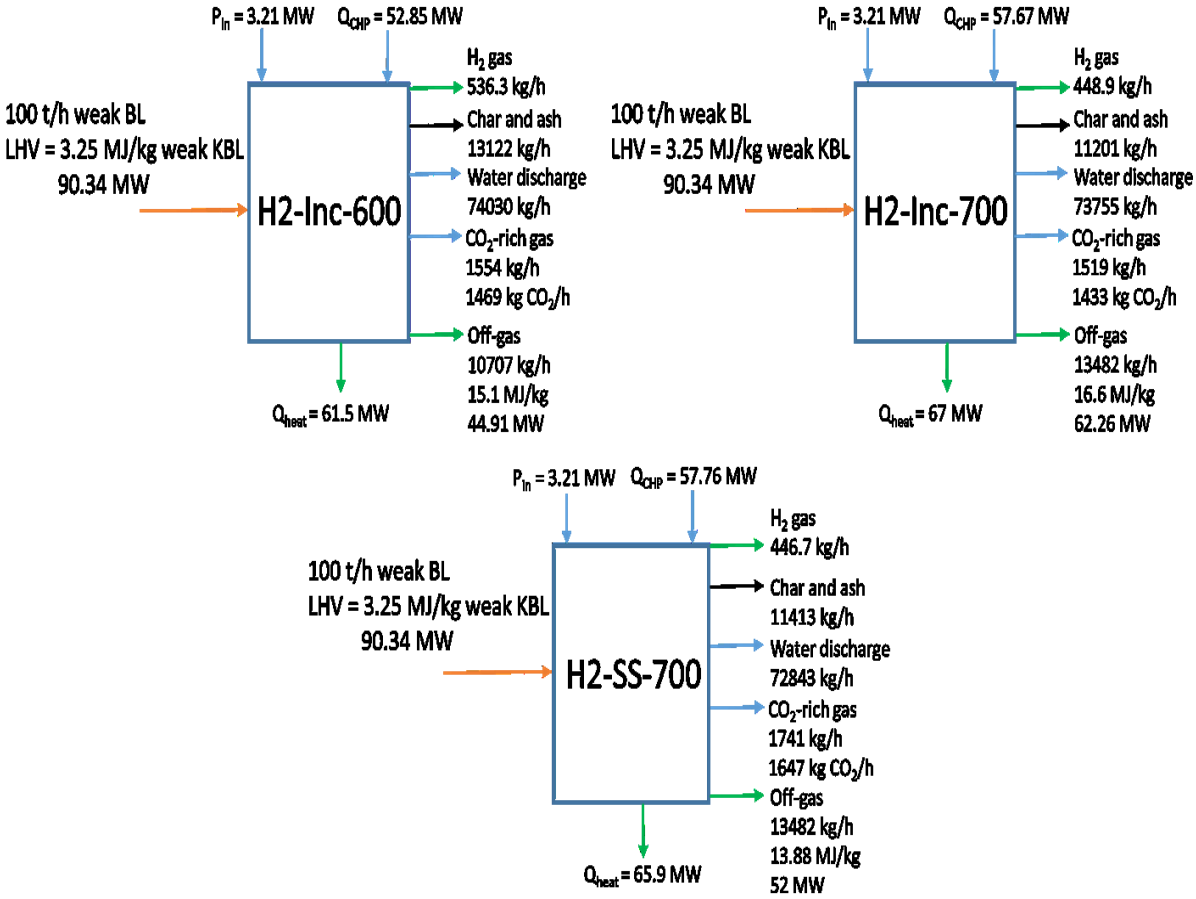

Figure 5. Input-output diagram for the hydrogen production scenarios

4. Equipment Design and Economic Evaluation

The equipment design is based on the chemical engineering design formulas [29] and pricing is based on the cost engineering principles [30]. All the purchase equipment costs are updated to the year 2018 through chemical engineering plant cost indexes (CEPCI). Operating costs are

also calculated based on the rules of thumbs [31]. In addition, the prices are converted to euro by using euro/dollar currency as 0.88.

4.1. Equipment Sizing and Capital Costs

The process units include the reactors, pressure vessels for phase separations, heat exchangers and pumps. The reactor is scaled up proportional to the capacity and designed as vertical vessel to enable solid separation. The reactor configuration can be applied as in VERENA pilot plant to avoid the plugging issues. The liquid feedstock and recycling supercritical water enter the reactor from the top. After flowing downwards, gas flows upwards through a dip-tube located at the center of the reactor. Meanwhile, solid phase is separated from downwards. For all scenarios, both HPSEP and LPSEP have the diameter of six times the minimum allowable diameter calculated via the settling velocity and are equipped with demister pad. These units are sized based on the liquid hold-up time of ten minutes. Pumps are designed through the head and duty calculation [29]. The recycling liquid pumped by the "HPPUMP" is transported through 100 m of equivalent pipeline and two heat exchangers to the "SCWG" reactor unit. The black liquor feed pumped by the "HP-PUMP" passes through 5 m of equivalent pipeline and one heat exchanger to the reactor. The efficiency of pumps is assumed as 80 % and each heat exchanger is assumed to cause pressure drop of 200 kPa. The heat exchangers are designed as shell-and-tube type, and Table 7 shows the heat transfer coefficients [29]. The pressure swing adsorption is represented as a separator to split the hydrogen and off-gas: "PSA" unit. The design of PSA is simplified based on a study investigating hydrogen purification from a gas mixture similar to syngas [32]: four columns with the recovery of 52 % and productivity of 59.9 mol H_2/kg adsorbent/day. The columns contain layered beds with activated carbon and zeolite with equal volumes.

Table 7. The heat transfer coefficients of heat exchangers in W/m^2 °C

	h1	**h2**	**U**
PRODCOOL	1500 (dilute aqueous)	1800 (dilute aqueous)	818.2
SYNEFF	2200 (condensed aqueous and dilute aqueous)	1800 (dilute aqueous)	990
HEATREAC	2000 (gas at high pressure and condensation of aqueous vapor)	2000 (boiling aqueous)	1000

Table 8 shows the equipment sizes. The reactors are designed as two parallel and identical reactors to which the inlet flow is split equally. The pumps are designed as multistage pumps [29]. The heat exchangers with more than 1000 m^2 area are designed as series heat exchangers with equally split area.

Table 8. Equipment list and design

Equipment	CHP-Inc-700	CHP-SS-700	H2-Inc-600	H2-Inc-700	H2-SS-700
SCWG	V_{total}: 121.2 m^3 H/D: 11.55 D: 1.88 m L: 21.75 m 2 in parallel	V_{total}: 121.2 m^3 H/D: 11.55 D: 1.88 m L: 21.75 m 2 in parallel	V_{total}: 121.2 m^3 H/D: 11.55 D: 1.88 m L: 21.75 m 2 in parallel	V_{total}: 121.2 m^3 H/D: 11.55 D: 1.88 m L: 21.75 m 2 in parallel	V_{total}: 121.2 m^3 H/D: 11.55 D: 1.88 m L: 21.75 m 2 in parallel
HPSEP	H: 14.28 m D: 2.67 m V: 79.68 m^3	H: 14.20 m D: 2.67 m V: 79.79 m^3	H: 15.12 m D: 2.54 m V: 76.46 m^3	H: 14.28 m D: 2.67 m V: 79.68 m^3	H: 14.20 m D: 2.67 m V: 79.79 m^3
LPSEP	H: 13.99 m D: 2.73 m V: 81.79 m^3	H: 13.06 m D: 2.92 m V: 87.24 m^3	H: 13.83 m D: 2.76 m V: 82.71 m^3	H: 13.99 m D: 2.73 m V: 81.79 m^3	H: 13.06 m D: 2.92 m V: 87.24 m^3
HPPUMP	Centrifugal P_{total}: 2.32 MW h_{total}: 2816 m ύ: 254 m^3/h Multistage	Centrifugal P_{total}: 2.32 MW h_{total}: 2816 m ύ: 254 m3/h Multistage	Centrifugal P_{total}: 2.32 MW h_{total}: 2815 m ύ: 253 m^3/h Multistage	Centrifugal P_{total}: 2.32 MW h_{total}: 2816 m ύ: 254 m^3/h Multistage	Centrifugal P_{total}: 2.32 MW h_{total}: 2816 m ύ: 253 m^3/h Multistage
HP-PUMP	Centrifugal P_{total}: 0.89 MW h_{total}: 2581 m ύ: 103 m^3/h Multistage	Centrifugal P_{total}: 0.89 MW h_{total}: 2581 m ύ: 103 m^3/h Multistage	Centrifugal P_{total}: 0.89 MW h_{total}: 2581 m ύ: 103 m^3/h Multistage	Centrifugal P_{total}: 0.89 MW h_{total}: 2581 m ύ: 103 m^3/h Multistage	Centrifugal P_{total}: 0.89 MW h_{total}: 2581 m ύ: 103 m^3/h Multistage
PRODCOOL	Q: 22.43 MW A: 415 m^2	Q: 22.42 MW A: 416 m^2	Q: 21.43 MW A: 392 m^2	Q: 22.43 MW A: 415 m^2	Q: 22.42 MW A: 414 m^2
SYNEFF	Q: 97.80 MW A: 1656 m^2 2 in series	Q: 97.60 MW A: 1670 m^2 2 in series	Q: 93.80 MW A: 1675 m^2 2 in series	Q: 97.80 MW A: 1656 m^2 2 in series	Q: 97.60 MW A: 1670 m^2 2 in series
HEATREAC	Q: 141.3 MW A: 5602 m^2 6 in series	Q: 141.5 MW A: 5592 m^2 6 in series	Q: 126.1 MW A: 4789 m^2 5 in series	Q: 141.3 MW A: 5602 m^2 6 in series	Q: 141.5 MW A: 5592 m^2 5 in series
PSA	-	-	4 columns V_{total}: 54.17 m^3 AC_{total}: 45.6 ton $Zeolite_{total}$: 61.0 ton	4 columns V_{total}: 45.34 m^3 AC_{total}: 38.2 ton $Zeolite_{total}$: 51.0 ton	4 columns V_{total}: 45.12 m^3 AC_{total}: 38.0 ton $Zeolite_{total}$: 50.8 ton

The purchasing costs are shown in Table 9. The differences in purchasing cost result mainly from the cost of reactor materials. The material factors were given as 1.4 for stainless steel and 3.4 for Inconel 600 for purchase cost of equipment cost [30]. The material factor of Inconel 625 is adjusted as 4.06 based on the relative price of Inconel 625 to Inconel 600 [33].

Table 9. The equipment purchase costs in 2018 in M€

Equipment	CHP-Inc-700	CHP-SS-700	H2-Inc-600	H2-Inc-700	H2-SS-700
SCWG	5.614	1.936	5.614	5.614	1.936
HPSEP	1.173	1.174	1.139	1.173	1.174
LPSEP	0.137	0.143	0.138	0.137	0.143
HPPUMP	0.615	0.615	0.615	0.615	0.615
HP-PUMP	0.333	0.333	0.333	0.333	0.333
PRODCOOL	0.378	0.379	0.364	0.378	0.378
SYNEFF	1.203	1.210	1.212	1.203	1.210
HEATREAC	3.910	3.906	3.315	3.910	3.906
PSA	-	-	0.203	0.177	0.176
Total production cost	13.4	9.7	12.9	13.5	9.9

Table 10 shows the total capital investments: calculated as the sum of fixed capital investment and working capital, as in Equation 1. The fixed capital investment is calculated by multiplying the purchase cost of equipment with two factors as shown in Equation 2 [29]. The first factor represents the physical plant cost including equipment erection, piping, instrumentation and buildings. The second factor represents the costs of engineering, supervision, contract fee and contingency. Then, the working capital represents the cost of one-month operating cost before the first sales, as shown in Equation 3. (Operating costs are determined in the next subsection.)

$$Total\ Capital\ Investment = Fixed\ capital\ investment + Working\ capital \quad (1)$$

$$Fixed\ capital\ investment = Purchase\ cost\ of\ equipment\ x\ 3.15\ x\ 1.40 \quad (2)$$

$$Working\ capital = Annual\ operating\ cost/12 \quad (3)$$

Table 10. Investment costs in 2018

Scenario	Fixed capital investment (M€)	Working capital (M€)	Total capital investment (M€)
CHP-Inc-700	58.9	5.2	64.1
CHP-SS-700	42.7	5.0	47.8
H2-Inc-600	57.0	4.9	61.9
H2-Inc-700	59.7	5.2	64.9
H2-SS-700	43.5	5.0	48.5

4.2. Operating Costs and Revenues

Operating costs comprise variable and fixed costs. The variable costs include raw material, electricity for pumps, heat from flue gas and operating supplies. The fixed costs include labor, employee social benefits, supervision, laboratory, insurance and taxes, maintenance and plant overhead. It is assumed that CHP process generates energy as 30 % electricity and 70 % heat. With the electricity price of 75 €/MWh [34] and the district heat price of 60 €/MWh [35], the weighted average is 64.5 €/MWh as the price of energy associated with the heating value of black liquor and flue gas. The operating supplies, maintenance, insurance and taxes, and plant overhead costs are assumed to be 1 %, 6 %, 3 % and 1 % of the fixed capital costs, respectively [29]. Labor is calculated based on two operators per shift based on the equipment of the plant [31], with the salary of 3000 €/month and three shifts per day, besides a manager with the salary of 5000 €/month. Employee social benefits, supervision and laboratory costs are 40 %, 30 % and 10 % of the labor cost, respectively [29].

The black liquor cost is calculated based on the functionality and operation in the commercial treatment, as shown in Table 11. The amount of heat to concentrate black liquor is calculated based on steam economy information in the evaporation step [36]. Then, the cost of evaporation is calculated by multiplying this heat amount with the district heat price. In addition, it is assumed that 5 % of solid content also evaporates in the evaporation step [37]. The air amount and the heat amount to preheat air and black liquor were given based on the industrial recovery boilers [37]. The given price of air for 1998 was updated to the current price through CEPCI indexes [29]. The prices of cooking chemicals were obtained from the indicative chemical price

list [38]. It is assumed that the cooking chemicals can be recovered by recycling the solid outlet to the recovery boiler. Nevertheless, Table 11 also shows inserting cost of cooking chemical loss, used in the sensitivity analysis in case of incomplete recovery. The amounts of cooking chemicals are calculated from the black liquor content.

Table 11. The cost of weak black liquor: 1 kg of weak black liquor as the basis

Commercial treatment operation	**Remarks**	**Material and energy needed or produced**	**Contribution to the black liquor price**
Evaporation	Moisture down to 20 % In: 0.228 kg solid, 0.772 kg water Out: 0.217 kg solid, 0.054 kg water	325 kJ heat needed	-0.00542
Recovery boiler	In: 0.217 kg solid, 0.054 kg water 13.6 MJ/kg dry solid 88.5 % efficiency of steam gen.	1.26 kg air needed 89.6 kj preheating air 3.04 kj preheating BL 2.95 MJ	-0.01097 -0.001494 -0.00005063 0.04679
Chemical loss	Make-up to the digester 0.451 €/kg Na_2S, 0.133 €/kg NaOH	0.037 kg Na_2S 0.012 kg NaOH	(0.01828) x loss fraction
Price of weak black liquor		0.02887 + (0.01828 x loss fraction)	

Operating costs are listed in Table 12. The main operating costs are black liquor and heat from flue gas. The H2-Inc-600 scenario has slightly lower cost of heat from flue gas due to lower reaction temperature. The scenarios with Inconel 625 reactors have slightly higher costs in the expenses linked to the investment costs, such as maintenance and insurance.

Table 12. Operating costs for all scenarios in M€/year in 2018 basis

	CHP-Inc-700	**CHP-SS-700**	**H2-Inc-600**	**H2-Inc-700**	**H2-SS-700**
Black liquor	23.09	23.09	23.09	23.09	23.09
Operating supplies	0.59	0.43	0.57	0.59	0.43
Heat from flue gas	29.76	29.80	27.27	29.76	29.80
Electricity	1.93	1.93	1.93	1.93	1.93
Labor	0.28	0.28	0.28	0.28	0.28
Employee social benefits	0.11	0.11	0.11	0.11	0.11
Supervision	0.083	0.083	0.083	0.083	0.083
Laboratory	0.028	0.028	0.028	0.028	0.028
Insurance & tax	1.77	1.28	1.71	1.79	1.28
Maintenance	3.54	2.57	3.42	3.58	2.57
Plant overhead	0.59	0.43	0.57	0.60	0.43
Total operating cost	61.8	60.0	59.1	61.8	60.1

The revenues are calculated based on the functionality of product gases. For the energy production scenarios, the revenue involves the heating value in H_2-rich gas and the excess district heat. For the hydrogen production scenarios, the revenue involves hydrogen in H_2 stream, off-gas used for CHP production and the excess district heat. Equations 4 and 5 show the revenue calculation for the energy and hydrogen production scenarios, respectively:

$$Rev_{CHP} = (\dot{m} * LHV)_{H2-rich}\, x\, 64.5\,\frac{€}{MWh} + Q_{heat}\, x\, 60\,\frac{€}{MWh} \quad (4)$$

$$Rev_{H2} = \dot{m}_{H2}\, x\, Price_{H_2}\,\frac{€}{kg\, H_2} + Q_{heat}\, x\, 60\,\frac{€}{MWh} + (\dot{m} * HV)_{Offgas}\, x\, 64.5\,\frac{€}{MWh} \quad (5)$$

where ṁ represents mass flow rate, LHV represents the lower heating value and Q_{heat} represents the excess heat rate as shown in Figures 3 and 5.

Table 13. Revenues in M€/year in the year 2018

Scenario	H_2-rich gas	H_2	Off-gas	Excess heat	Total Revenue
CHP-Inc-700	39.8	-	-	32.2	72.0
CHP-SS-700	34.4	-	-	31.6	66.0
H2-Inc-600	-	13.7	23.2	29.5	66.4
H2-Inc-700	-	5.2	32.1	32.2	69.5
H2-SS-700	-	7.2	26.8	31.6	65.7

Table 13 determines the revenue for all scenarios. The energy production scenario with the Inconel reactor have slightly more revenue due to higher yields than stainless steel reactor. For the hydrogen production scenarios, the manufacturing cost of hydrogen is determined by setting 20-year NPV to zero and used as the price of hydrogen in the revenue calculation. The manufacturing cost of hydrogen is 3.193 €/kg H_2 for the H2-Inc-600 scenario, 1.456 €/kg H_2 for the H2-Inc-700 scenario and 2.073 €/kg H_2 for the H2-SS-700 scenario.

4.3. Profitability

Profitability is evaluated based on net present value (NPV) and internal rate of return (IRR) for the energy production scenarios. For the hydrogen production scenarios, the manufacturing cost of hydrogen is calculated by setting NPV to zero at the project end time. The project lifetime is considered as 20 years with straight line depreciation model. The investment is applied in the year 0 and the operation starts in the year 1. The interest rate is assumed as 2 % for the investment cost, and the discount factor is assumed as 5 %. Equations 6-13 give the formulation net present value calculation.

$$Earning\ before\ interest\ and\ tax\ (EBIT) = Revenue - Operating\ Cost \quad (6)$$

$$Depreciation = 0.05\, x\, Total\ Capital\ Investment \quad (7)$$

$$Profit\ before\ tax = EBIT - Depreciation \quad (8)$$

$$Interest = 0.02\, x\, Total\ Capital\ Investment \quad (9)$$

$$Tax = 0.25\, x\, Profit\ before\ tax \quad (10)$$

$$Profit\ after\ tax = Profit\ before\ tax - Tax - Interest \quad (11)$$

$$Net\ Present\ Value_0 = -Total\ Capital\ Investment \quad (12)$$

$$NPV_n = NPV_{n-1} + (Profit\ after\ tax + Depreciation)/(1 + 0.05)^n \quad (13)$$

Figure 6 shows the NPV and IRR for the energy production scenarios and the hydrogen manufacturing costs for the hydrogen production scenarios. For the energy production, both scenarios give positive NPV and reasonably good IRR whereas CHP-Inc-700 scenario gives

higher NPV and IRR. For the hydrogen production scenarios, the highest production cost is obtained in Inconel reactor at 600 °C despite the highest hydrogen yield, due to lower revenue from the off-gas. In contrast, despite low hydrogen yield, the lowest production cost is obtained in Inconel reactor at 700 °C because of higher revenue from the off-gas.

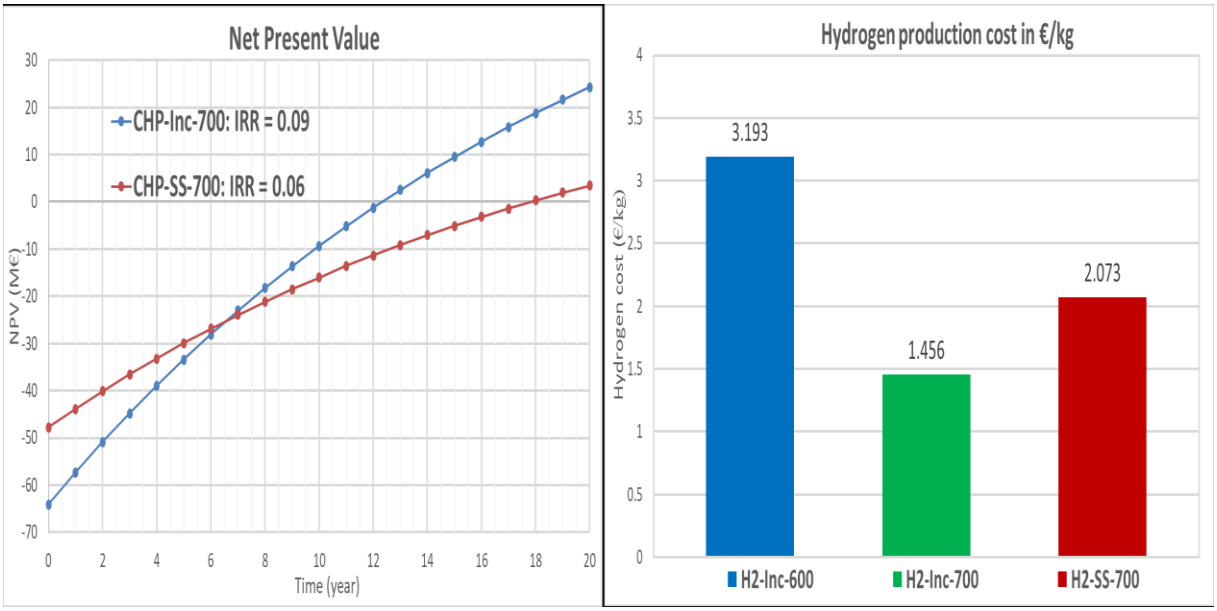

Figure 6. The profitability of the energy production scenarios and manufacturing costs for the hydrogen production scenarios

4.4. Sensitivity

The two critical aspects are the energy prices and cooking chemical loss, investigated for the sensitivity analysis. The sensitivity analysis on energy prices assumes that the heat and electricity price changes simultaneously with the same rate, thus changing the CHP price in the same rate. The chemical loss is reflected on the black liquor cost based on the loss fraction.

The sensitivity results presented in Figures 7 and 8 show that Inconel reactor is more robust against the changes in energy prices and chemical loss. In addition, the CHP-Inc-700 scenario maintains positive NPV up to 15 % chemical loss while the CHP-SS-700 scenario has negative NPV in case of any chemical loss.

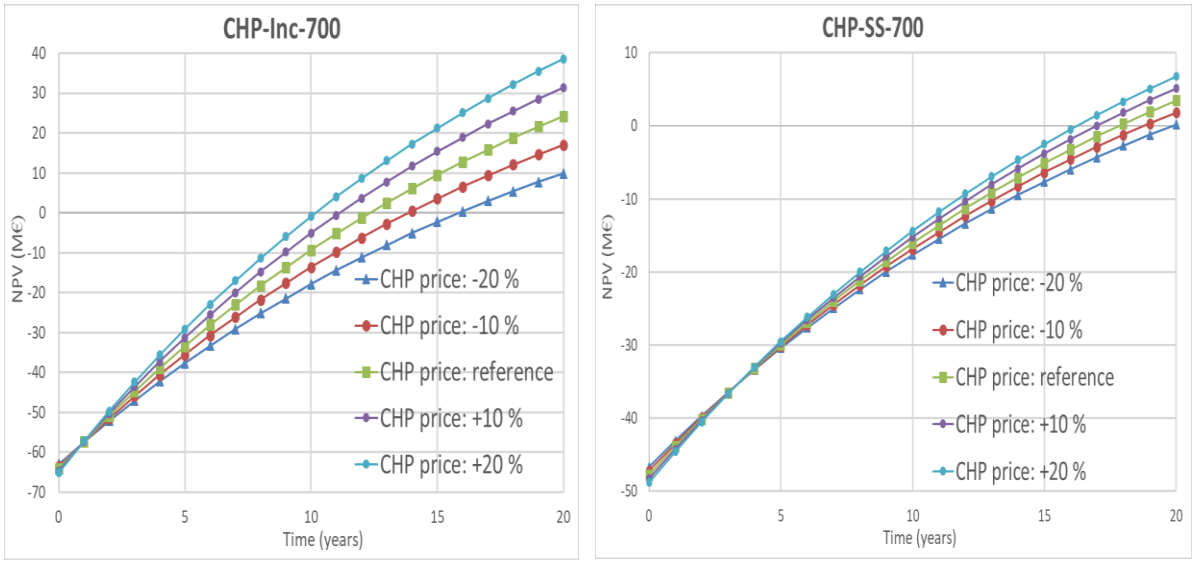

Figure 7. The sensitivity towards change in energy price for the energy production scenarios

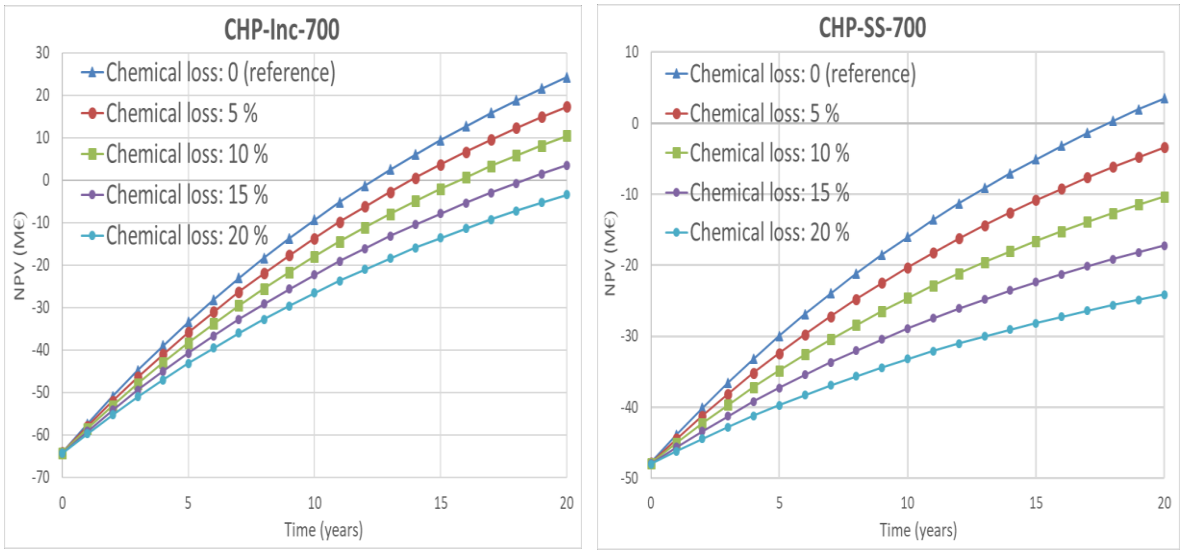

Figure 8. The sensitivity towards cooking chemical loss for the energy production scenarios

Figure 9 shows the sensitivity analysis for the hydrogen production scenarios. The chemical loss influences sharply all scenarios although the scenarios with Inconel reactor are slightly more robust. The production cost increases with increasing energy prices, except for the H2-Inc-700 scenario. The production cost increases with increasing energy prices, except for the H2-Inc-700 scenario. The increase in energy prices increases the costs of black liquor and heating the recycled SCW while increasing the revenue from off-gas as well. The sensitivity results on energy prices show that the operation costs are more intensively influenced than the revenue through off-gas. However, the H2-Inc-700 scenario has higher CHP outcome through off-gas than other scenarios. With increasing energy price in the H2-Inc-700 scenario, the additional revenue from off-gas is able to compensate the additional operational costs, thus maintaining the production cost robust.

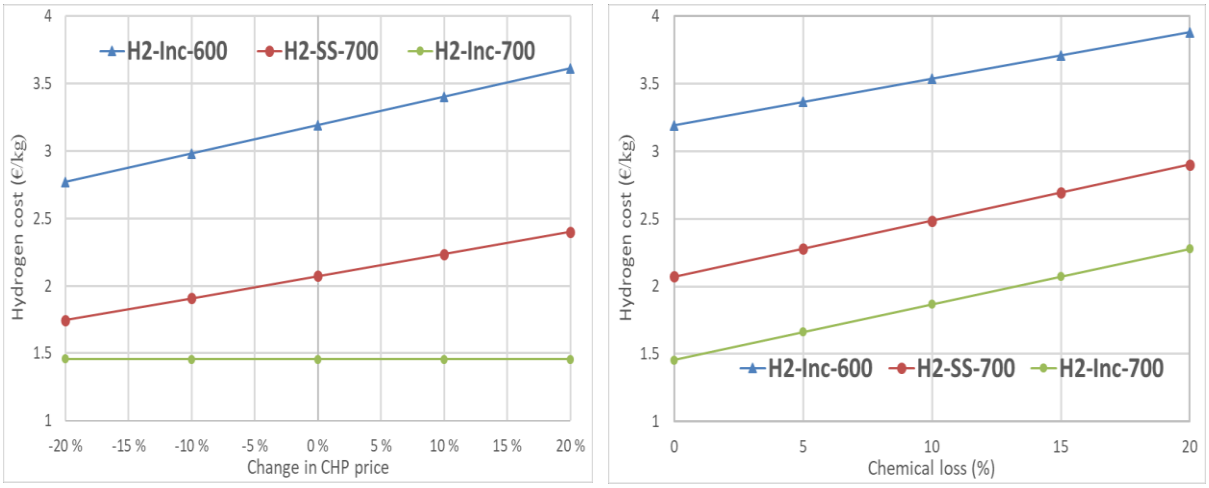

Figure 9. The sensitivity analysis for the hydrogen production scenarios

4.5. Future Aspects and Implementation

This study performs conceptual feasibility assessment useful for the initial evaluation and comparison of process alternatives. Since this methodology involves 30-50 % inaccuracy; for the implementation purpose, the techno-economic assessment should be repeated including rigorous models and the current market data for the simplified aspects. In addition, this study assumes the same yields with experiments by scaling up the reactor proportionally to the inlet flow rates. This aspect should also be confirmed with pilot scale operations before industrial implementation. Since Inconel has more catalytic impact, the surface-to-volume ratio influences the gas yields [39]. Although a large vessel does not provide as high surface-to-volume ratio as lab-scale tubular reactors, the reactor design can involve some special improvements on this regard, such as multiple, coil-shaped dip-tubes.

From the simulation viewpoint, a future scope can be representing the properties of biomass with non-conventional components for the applications with more concentrated biomass streams. The simulation studies of SCWG were mostly conducted for conventional compounds, such as methanol [40], glycerol [41] and model compounds of lignocellulosic biomass including glucose [40] and phenol [41]. These simulations involve Gibbs reactor minimizing the Gibbs free energy of the system for the equilibrium simulations. Gibbs free energy minimization can give consistent results with experiments for conventional compounds [42]. However, non-conventional compounds are more complicated, and the reactions might not reach equilibrium in a reasonable residence time for industrial implementation. For instance, lignin and phenol are challenging substances on this regard. For the equilibrium simulations, the reactor is represented as the unit decomposing the biomass stream into elements followed by Gibbs reactor minimizing the Gibbs free energy of the system [41]. However, this is usually mismatching with the experiments in gasification and SCWG applications. This mismatch results from very rough representation of non-conventional compounds and some reactions having kinetics limitation (such as water-gas-shift reaction in the absence of alkali metal). In addition, kinetic modeling of biomass conversion has also some

weaknesses due to the complexity: lacking the whole conversion route, lumped models, assuming 1st order reactions and insufficient representation of temperature effect on rate constants [43].

Regarding the integration of SCWG to a pulp mill, Inconel is more efficient for both energy and hydrogen production. In addition, the reactors can operate adiabatically since thick walls due to high pressure can reduce the heating efficiency. Since the heating rate is influential on tar and char formation [44], adiabatic operation would address the undesired impacts of slow heating rate as well.

SCWG can be an attractive treatment especially for non-wood mills. The non-wood black liquor has currently no commercial treatment, causing environmental issues when discharging or even plant shut down. SCWG can provide a treatment solution: processing the whole black liquor. However, this also means that there is no infrastructure of CHP and turbines, thus requiring extra investment. As an advantage, non-wood black liquor has more hemicellulose and less lignin compared to KBL, thus implying less char and tar formation. For instance, SCWG of wheat straw black liquor was investigated under various feed concentration and residence time [18,45].

The results of techno-economic assessment can be improved by determining the optimum conditions based on comprehensive investigations. Further investigations can include residence time in the reactor, catalysts, the flow regime and concentration of the reactor inlet. For instance, lowering reactor inlet concentration provides higher thermal efficiency and hydrogen yield; however, this would require more CHP in the process operation due to higher amount of recycling SCW. Nevertheless, catalysts can enable sufficient yields at lower temperature, thus reducing the CHP need on the recycling SCW. Besides the alkali content in black liquor acting as homogeneous catalysts, transition metal catalysts can promote the gas yields as heterogeneous catalysts. Nickel catalysts have low cost while ruthenium is very active even with low metal loading [46]. For instance, PSI process operates at 400-450 °C with Ru/C catalyst [27]. Furthermore, the impact of a process condition depends on the set of conditions. For instance, Inconel reactor promotes gas yields intensively compared with stainless steel at high temperatures (600 °C or above) while stainless steel can be more effective at lower temperatures around 400-500 °C [47]. From the raw material viewpoint, the integrated SCWG process in a pulp mill can process the wastes of other sectors as well. SCWG has been investigated for biomass types from other sectors as well: manure [48], algae [49], glycerol [50], sewage sludge [51,52], fruit pulp [53], olive mill wastewater [54] and fermentation residues [55].

The main obstacles for industrial application include high amount of char and solid deposition resulting in plugging. The comprehensive studies can be useful for determining the conditions with minimum char formation as well. Other measures of suppressing char formation include bimetallic catalyst and phenol addition. Phenol addition ensures dissolution of all lignin

fraction and hinders repolymerization [28] despite decreasing the gasification of sugars [56,57]. Nevertheless, phenol addition can be beneficial for SCWG of black liquor because of high content of lignin fractions. Bimetallic catalyst can improve the process via different roles in the reaction mechanism. For instance, nickel promotes decomposition and gas phase reactions, cobalt inhibits repolymerization, and Mg-Al support promotes depolymerization and fragmentation [58]. Therefore, nickel-cobalt catalyst with magnesium-aluminum support (Ni-Co/Mg-Al) improved gas yields with reduced char formation [58]. The solid deposition is an issue also due to inorganic salts despite the possible reductions in char formation. Since alkali metals promote the reactions, a solution can be a special reactor configuration enabling simultaneous separation of solids, e.g. as in Verena pilot plant [26]. Alternatively, a salt separator prior to the reactor can prevent catalyst poisoning in the reactor by removing Sulphur content. A salt separator with dip-tube or riser-tube configuration can operate slightly over the critical temperature with very short residence in the magnitude of seconds [59]. For instance, catalytic VERENA setup operated without any issue for glycerol and digestate sludge feedstocks, with a salt separator followed by a ZnO and Ru/C layered fixed-bed reactor [60].

The long-term operational aspects include catalyst deactivation and corrosion. The deactivation can result from sintering of the heterogeneous catalysts [46] and the adsorption of intermediates to the catalyst surface [61]. Nevertheless, bimetallic catalyst promotion can address this issue because of promoting decomposition and suppressing repolymerization. Dispersion of the active site on the support was also investigated as a key parameter for deactivation through a study on ruthenium catalyst: the higher dispersion is the more improved stability of catalyst as well as reduced char formation [62]. In addition, alkali catalysts can be improved regarding activity and lifetime by adding trace amounts of transition metals [63]. Therefore, Inconel reactor wall can have longer lifetime as the alloy of nickel, chromium and molybdenum. Corrosion is another aspect for industrial implementation. SCWG has much less issue of electrochemical corrosion than hot compressed water around critical point since radical reaction mechanism is dominant at high temperature, rather than ionic mechanism. Some other corrosion forms can occur as dealloying due to sulfide and under-deposit corrosion due to salt fouling [64]. Despite some studies observing corrosion on Nickel alloys at high temperatures [65], the reviews reported stainless steel and Nickel alloys as corrosion resistant materials [64,66]. Moreover, the pilot plant in Hiroshima operates at 600 °C without any corrosion issue, made of stainless steel reactor [25].

Furthermore, the process can be improved when integrated to a pulp mill with LignoForce process, PWO of black liquor and lignin recovery by acidification. In addition, two parallel reactors can operate also for syngas and bio-oil as the target products. PWO downstream can be split between lignin recovery section, SCWG and HTL. This integration will increase the product spectrum further: lignin, bio-oil, hydrogen and CHP. PWO oxidizes sulphur and potentially prevents sulphur content in syngas, thus eliminating the need of gas cleaning operation [67]. This would also prevent dealloying of the reactor wall due to sulphide.

However, more experimental data are needed for this type of multi-product process, e.g. HTL and SCWG of PWO downstream.

In terms of sustainable biorefinery, it is economically more feasible to utilize all the waste streams from biomass sectors than processing a single feedstock. Sectoral integration was proposed as the biomass supply chain network [67]: pre-treatment in the biomass site, multi-feed-multi-product processes as regional conversion and the central upgrading of the intermediates. In this concept, the process can be integrated to a pulp mill as a regional conversion process receiving other waste streams as well. This can improve both economic and environmental performance of agriculture and aquaculture sectors as well as pulp and paper industry.

5. Conclusion

This study investigates the feasibility of SCWG of Kraft black liquor integrated with a pulp mill, considering the potential opportunity to evolve pulp mill to multi-product biorefinery. The process is designed based on the experimental results and the purpose of product gases. The main expenses of the process are raw material cost and the cost of heat from flue gas. In addition, there is excess heat as an additional revenue source. Based on the present analysis, Inconel reactor is more profitable than the stainless steel reactor for both energy production and hydrogen production. In addition, the Inconel reactor is more robust against loss of pulping chemicals in SCWG process and variations in energy prices. On the other hand, these results require further validation during scale-up versus surface-to-volume ratio of the reactor due to the uncertainty in catalytic effect of the reactor material.

SCWG can have further applications as well: a treatment option for non-wood mill or a regional biomass conversion process. These applications require experimental data and economic analysis with various biomass types. Nevertheless, since all types of biomass have high moisture content, hydrothermal processes become more suitable for biomass conversion.

Acknowledgement

The authors would like to thank School of Chemical Engineering in Aalto University, TES (Tekniikan edistämissäätiö – Finnish Foundation for Technology Promotion) and Åbo Akademi University for funding the work resulting in this manuscript.

References

[1] Balat M, Balat M, Kırtay E, Balat H. Main routes for the thermo-conversion of biomass into fuels and chemicals. Part 1: Pyrolysis systems. Energy Convers Manag 2009;50:3147–57. doi:10.1016/j.enconman.2009.08.014.

[2] Balat M, Balat M, Kırtay E, Balat H. Main routes for the thermo-conversion of biomass into fuels and chemicals. Part 2: Gasification systems. Energy Convers Manag 2009;50:3158–68. doi:10.1016/j.enconman.2009.08.013.
[3] Akin O, Yuksel A. Novel hybrid process for the conversion of microcrystalline cellulose to value-added chemicals: part 2: effect of constant voltage on product selectivity. Cellulose 2017;24:4729–41. doi:10.1007/s10570-017-1457-9.
[4] Akin O, Yuksel A. Novel hybrid process for the conversion of microcrystalline cellulose to value-added chemicals: part 1: process optimization. Cellulose 2016;23:3475–93. doi:10.1007/s10570-016-1054-3.
[5] Yuksel A, Koga H, Sasaki M, Goto M. Hydrothermal Electrolysis of Glycerol Using a Continuous Flow Reactor. Ind Eng Chem Res 2010;49:1520–5. doi:10.1021/ie9016418.
[6] Forest-based energy. Finn For Assoc 2016. https://smy.fi/en/forest-fi/forest-facts/forest-based-energy/ (accessed April 15, 2019).
[7] Tomani P. The LignoBoost process. Cellul Chem Technol 2010;44:53–8.
[8] Kouisni L, Gagné A, Maki K, Holt-Hindle P, Paleologou M. LignoForce System for the Recovery of Lignin from Black Liquor: Feedstock Options, Odor Profile, and Product Characterization. ACS Sustain Chem Eng 2016;4:5152–9. doi:10.1021/acssuschemeng.6b00907.
[9] Naqvi M, Yan J, Dahlquist E. Black liquor gasification integrated in pulp and paper mills: A critical review. Bioresour Technol 2010;101:8001–15. doi:10.1016/j.biortech.2010.05.013.
[10] Pettersson K, Harvey S. Comparison of black liquor gasification with other pulping biorefinery concepts – Systems analysis of economic performance and CO2 emissions. Energy 2012;37:136–53. doi:10.1016/j.energy.2011.10.020.
[11] Brammer JG, Bridgwater AV. The influence of feedstock drying on the performance and economics of a biomass gasifier–engine CHP system. Biomass Bioenergy 2002;22:271–81. doi:10.1016/S0961-9534(02)00003-X.
[12] Saidur R, BoroumandJazi G, Mekhilef S, Mohammed HA. A review on exergy analysis of biomass based fuels. Renew Sustain Energy Rev 2012;16:1217–22. doi:10.1016/j.rser.2011.07.076.
[13] Yoshida Y, Dowaki K, Matsumura Y, Matsuhashi R, Li D, Ishitani H, et al. Comprehensive comparison of efficiency and CO2 emissions between biomass energy conversion technologies—position of supercritical water gasification in biomass technologies. Biomass Bioenergy 2003;25:257–72. doi:10.1016/S0961-9534(03)00016-3.
[14] Tekin K, Karagöz S, Bektaş S. A review of hydrothermal biomass processing. Renew Sustain Energy Rev 2014;40:673–87. doi:10.1016/j.rser.2014.07.216.
[15] Muddassar HR, Melin K, de Villalba Kokkonen D, Riera GV, Golam S, Koskinen J. Green chemicals from pulp production black liquor by partial wet oxidation. Waste Manag Res J Int Solid Wastes Public Clean Assoc ISWA 2015;33:1015–21. doi:10.1177/0734242X15602807.
[16] Özdenkçi K, Koskinen J, Sarwar G. Recovery of sodium organic salts from partially wet oxidized black liquor. Cellul Chem Technol 2014;48:825–33.
[17] De Blasio C, Lucca G, Özdenkci K, Mulas M, Lundqvist K, Koskinen J, et al. A study on supercritical water gasification of black liquor conducted in stainless steel and nickel-chromium-molybdenum reactors. J Chem Technol Biotechnol 2016;91:2664–78. doi:10.1002/jctb.4871.
[18] Cao C, Guo L, Chen Y, Guo S, Lu Y. Hydrogen production from supercritical water gasification of alkaline wheat straw pulping black liquor in continuous flow system. Int J Hydrog Energy 2011;36:13528–35. doi:10.1016/j.ijhydene.2011.07.101.

[19] Sricharoenchaikul V. Assessment of black liquor gasification in supercritical water. Bioresour Technol 2009;100:638–43. doi:10.1016/j.biortech.2008.07.011.
[20] Cao C, Zhang Y, Li L, Wei W, Wang G, Bian C. Supercritical water gasification of black liquor with wheat straw as the supplementary energy resource. Int J Hydrog Energy 2018. doi:10.1016/j.ijhydene.2018.10.006.
[21] Rönnlund I, Myréen L, Lundqvist K, Ahlbeck J, Westerlund T. Waste to energy by industrially integrated supercritical water gasification – Effects of alkali salts in residual by-products from the pulp and paper industry. Energy 2011;36:2151–63. doi:10.1016/j.energy.2010.03.027.
[22] Kruse A, Dahmen N. Water – A magic solvent for biomass conversion. J Supercrit Fluids 2015;96:36–45. doi:10.1016/j.supflu.2014.09.038.
[23] Sasaki M, Kabyemela B, Malaluan R, Hirose S, Takeda N, Adschiri T, et al. Cellulose hydrolysis in subcritical and supercritical water. J Supercrit Fluids 1998;13:261–8. doi:10.1016/S0896-8446(98)00060-6.
[24] Yong TL-K, Matsumura Y. Reaction Kinetics of the Lignin Conversion in Supercritical Water 2012. doi:10.1021/ie300921d.
[25] Matsumura Y. Chapter 9 - Hydrothermal Gasification of Biomass. In: Pandey A, Bhaskar T, Stöcker M, Sukumaran RK, editors. Recent Adv. Thermo-Chem. Convers. Biomass, Boston: Elsevier; 2015, p. 251–67. doi:10.1016/B978-0-444-63289-0.00009-0.
[26] Boukis N, Galla U, Müller H, Dinjus E, Box PO. BIOMASS GASIFICATION IN SUPERCRITICAL WATER. EXPERIMENTAL PROGRESS ACHIEVED WITH THE VERENA PILOT PLANT. 2007:4.
[27] Vogel F. Hydrothermal Conversion of Biomass. In: Meyers RA, editor. Encycl. Sustain. Sci. Technol., New York, NY: Springer New York; 2017, p. 1–46. doi:10.1007/978-1-4939-2493-6_993-1.
[28] Fang Z, Sato T, Smith RL, Inomata H, Arai K, Kozinski JA. Reaction chemistry and phase behavior of lignin in high-temperature and supercritical water. Bioresour Technol 2008;99:3424–30. doi:10.1016/j.biortech.2007.08.008.
[29] Sinnott R. Chemical Engineering Design. vol. 6. 3rd ed. Elsevier; 2003.
[30] Brown T. Cost Engineering: Equipment Purchase Costs 2019. https://www.chemengonline.com/cost-engineering-equipment-purchase-costs/?printmode=1 (accessed July 10, 2019).
[31] Brown T. Engineering Economics and Economic Design for Process Engineers. 1 edition. Boca Raton: CRC Press; 2006.
[32] Ribeiro AM, Grande CA, Lopes FVS, Loureiro JM, Rodrigues AE. A parametric study of layered bed PSA for hydrogen purification. Chem Eng Sci 2008;63:5258–73. doi:10.1016/j.ces.2008.07.017.
[33] Inconel 600 price per kg, Alloy 625 price, Inconel 718 Price India. Steel Tubes India 2019. https://www.stindia.com/blog/inconel-alloy-600-625-718-price-per-kg-india.html (accessed July 11, 2019).
[34] Aalto University. Industrial electricity prices across Europe 2017. Statista 2019. https://www.statista.com/statistics/267068/industrial-electricity-prices-in-europe/ (accessed July 11, 2019).
[35] European District Heating Price Series. Energiforsk; 2016.
[36] Parviainen K, Jaakola H, Nurminen K. Chapter 2: Evaporation of black liquor. Chem. Pulping Part 2 Recovery Chem. Enegy. 2nd ed., Jyväskylä, Finland: Paper Engineers' Association; 2008.
[37] Vakkilainen E. Chapter 3: Recovery Boiler. Chem. Pulping Part 2 Recovery Chem. Energy. 2nd ed., Jyväskylä, Finland: Paper Engineers' Association; 2008.

[38] Indicative Chemical Prices. ICIS Explore n.d. https://www.icis.com/explore/chemicals/channel-info-chemicals-a-z/ (accessed May 12, 2018).
[39] Tuan Abdullah TA, Croiset E. Evaluation of an Inconel-625 Reactor and its Wall Effects on Ethanol Reforming in Supercritical Water. Ind Eng Chem Res 2014;53:2121–9. doi:10.1021/ie403305d.
[40] Withag JAM, Smeets JR, Bramer EA, Brem G. System model for gasification of biomass model compounds in supercritical water – A thermodynamic analysis. J Supercrit Fluids 2012;61:157–66. doi:10.1016/j.supflu.2011.10.012.
[41] Fiori L, Valbusa M, Castello D. Supercritical water gasification of biomass for H2 production: Process design. Bioresour Technol 2012;121:139–47. doi:10.1016/j.biortech.2012.06.116.
[42] Yakaboylu O, Harinck J, Smit KG, de Jong W. Supercritical Water Gasification of Biomass: A Thermodynamic Model for the Prediction of Product Compounds at Equilibrium State. Energy Fuels 2014;28:2506–22. doi:10.1021/ef5003342.
[43] Yakaboylu O, Harinck J, Smit KG, De Jong W. Supercritical Water Gasification of Biomass: A Literature and Technology Overview. Energies 2015;8:859–94. doi:10.3390/en8020859.
[44] Matsumura Y, Harada M, Nagata K, Kikuchi Y. Effect of Heating Rate of Biomass Feedstock on Carbon Gasification Efficiency in Supercritical Water Gasification. Chem Eng Commun 2006;193:649–59. doi:10.1080/00986440500440157.
[45] Cao C, Xu L, He Y, Guo L, Jin H, Huo Z. High-Efficiency Gasification of Wheat Straw Black Liquor in Supercritical Water at High Temperatures for Hydrogen Production. Energy Fuels 2017;31:3970–8. doi:10.1021/acs.energyfuels.6b03002.
[46] Guo Y, Wang SZ, Xu DH, Gong YM, Ma HH, Tang XY. Review of catalytic supercritical water gasification for hydrogen production from biomass. Renew Sustain Energy Rev 2010;14:334–43. doi:10.1016/j.rser.2009.08.012.
[47] Castello D, Rolli B, Kruse A, Fiori L. Supercritical Water Gasification of Biomass in a Ceramic Reactor: Long-Time Batch Experiments. Energies 2017;10:1734. doi:10.3390/en10111734.
[48] Cao W, Cao C, Guo L, Jin H, Dargusch M, Bernhardt D, et al. Hydrogen production from supercritical water gasification of chicken manure. Int J Hydrog Energy 2016;41:22722–31. doi:10.1016/j.ijhydene.2016.09.031.
[49] Bagnoud-Velásquez M, Brandenberger M, Vogel F, Ludwig C. Continuous catalytic hydrothermal gasification of algal biomass and case study on toxicity of aluminum as a step toward effluents recycling. Catal Today 2014;223:35–43. doi:10.1016/j.cattod.2013.12.001.
[50] Guo S, Guo L, Yin J, Jin H. Supercritical water gasification of glycerol: Intermediates and kinetics. J Supercrit Fluids 2013;78:95–102. doi:10.1016/j.supflu.2013.03.025.
[51] Chen Y, Guo L, Cao W, Jin H, Guo S, Zhang X. Hydrogen production by sewage sludge gasification in supercritical water with a fluidized bed reactor. Int J Hydrog Energy 2013;38:12991–9. doi:10.1016/j.ijhydene.2013.03.165.
[52] Ibrahim ABA, Akilli H. Supercritical water gasification of wastewater sludge for hydrogen production. Int J Hydrog Energy 2019;44:10328–49. doi:10.1016/j.ijhydene.2019.02.184.
[53] Elif D, Nezihe A. Hydrogen production by supercritical water gasification of fruit pulp in the presence of Ru/C. Int J Hydrog Energy 2016;41:8073–83. doi:10.1016/j.ijhydene.2015.12.005.

[54] Kıpçak E, Söğüt OÖ, Akgün M. Hydrothermal gasification of olive mill wastewater as a biomass source in supercritical water. J Supercrit Fluids 2011;57:50–7. doi:10.1016/j.supflu.2011.02.006.
[55] Zöhrer H, Vogel F. Hydrothermal catalytic gasification of fermentation residues from a biogas plant. Biomass Bioenergy 2013;53:138–48. doi:10.1016/j.biombioe.2012.12.030.
[56] Goodwin AK, Rorrer GL. Conversion of Xylose and Xylose−Phenol Mixtures to Hydrogen-Rich Gas by Supercritical Water in an Isothermal Microtube Flow Reactor. Energy Fuels 2009;23:3818–25. doi:10.1021/ef900227u.
[57] Weiss-Hortala E, Kruse A, Ceccarelli C, Barna R. Influence of phenol on glucose degradation during supercritical water gasification. J Supercrit Fluids 2010;53:42–7. doi:10.1016/j.supflu.2010.01.004.
[58] Kang K, Azargohar R, Dalai AK, Wang H. Hydrogen generation via supercritical water gasification of lignin using Ni-Co/Mg-Al catalysts. Int J Energy Res 2017;41:1835–46. doi:10.1002/er.3739.
[59] Reimer J, Peng G, Viereck S, De Boni E, Breinl J, Vogel F. A novel salt separator for the supercritical water gasification of biomass. J Supercrit Fluids 2016;117:113–21. doi:10.1016/j.supflu.2016.06.009.
[60] Boukis N, Hauer E, Herbig S, Sauer J, Vogel F. Catalytic gasification of digestate sludge in supercritical water on the pilot plant scale. Biomass Convers Biorefinery 2017;7:415–24. doi:10.1007/s13399-017-0238-x.
[61] Yoshida T, Oshima Y, Matsumura Y. Gasification of biomass model compounds and real biomass in supercritical water. Biomass Bioenergy 2004;26:71–8. doi:10.1016/S0961-9534(03)00063-1.
[62] Peng G, Ludwig C, Vogel F. Ruthenium Dispersion: A Key Parameter for the Stability of Supported Ruthenium Catalysts during Catalytic Supercritical Water Gasification. ChemCatChem 2016;8:139–41. doi:10.1002/cctc.201500995.
[63] Elliott DC, Hart TR, Neuenschwander GG. Chemical Processing in High-Pressure Aqueous Environments. 8. Improved Catalysts for Hydrothermal Gasification. Ind Eng Chem Res 2006;45:3776–81. doi:10.1021/ie060031o.
[64] Marrone PA, Hong GT. Corrosion control methods in supercritical water oxidation and gasification processes. J Supercrit Fluids 2009;51:83–103. doi:10.1016/j.supflu.2009.08.001.
[65] Antal MJ, Allen SG, Schulman D, Xu X, Divilio RJ. Biomass Gasification in Supercritical Water. Ind Eng Chem Res 2000;39:4040–53. doi:10.1021/ie0003436.
[66] Rodriguez Correa C, Kruse A. Supercritical water gasification of biomass for hydrogen production – Review. J Supercrit Fluids 2018;133:573–90. doi:10.1016/j.supflu.2017.09.019.
[67] Özdenkçi K, De Blasio C, Muddassar HR, Melin K, Oinas P, Koskinen J, et al. A novel biorefinery integration concept for lignocellulosic biomass. Energy Convers Manag 2017;149:974–87. doi:10.1016/j.enconman.2017.04.034.